Conserved arginine-516 of *Penicillium amagasakiense* glucose oxidase is essential for the efficient binding of β-D-glucose

Susanne WITT[1], Gerd WOHLFAHRT[2], Dietmar SCHOMBURG[2], Hans-Jürgen HECHT and Henryk M. KALISZ[3]
GBF (Gesellschaft für Biotechnologische Forschung), Mascheroder Weg 1, D-38124 Braunschweig, Germany

The effects of mutation of key conserved active-site residues (Tyr-73, Phe-418, Trp-430, Arg-516, Asn-518, His-520 and His-563) of glucose oxidase from *Penicillium amagasakiense* on substrate binding were investigated. Kinetic studies on the oxidation of β-D-glucose combined with molecular modelling showed the side chain of Arg-516, which forms two hydrogen bonds with the 3-OH group of β-D-glucose, to be absolutely essential for the efficient binding of β-D-glucose. The R516K variant, whose side chain forms only one hydrogen bond with the 3-OH group of β-D-glucose, exhibits an 80-fold higher apparent K_m (513 mM) but a V_{max} only 70% lower (280 units/mg) than the wild type. The complete elimination of a hydrogen-bond interaction between residue 516 and the 3-OH group of β-D-glucose through the substitution R516Q effected a 120-fold increase in the apparent K_m for glucose (to 733 mM) and a decrease in the V_{max} to 1/30 (33 units/mg). None of the other substitutions, with the exception of variant F418A, affected the apparent K_m more than 6-fold. In contrast, the removal of aromatic or bulky residues at positions 73, 418 or 430 resulted in decreases in the maximum rates of glucose oxidation to less than 1/90. Variants of the potentially catalytically active His-520 and His-563 were completely, or almost completely, inactive. Thus, of the residues forming the active site of glucose oxidase, Arg-516 is the most critical amino acid for the efficient binding of β-D-glucose by the enzyme, whereas aromatic residues at positions 73, 418 and 430 are important for the correct orientation and maximal velocity of glucose oxidation.

Key words: active site, kinetic studies, molecular modelling, site-directed mutagenesis.

INTRODUCTION

Glucose oxidase (GOX) is a flavoprotein that catalyses the oxidation of β-D-glucose by molecular oxygen to δ-gluconolactone and H_2O_2. GOX activity has been identified from various sources. However, only the enzymes from *Aspergillus niger* and *Penicillium amagasakiense*, which are of considerable commercial importance [1–3], have been studied in detail [4–13]. The main application of GOX is in biosensors, where it is used for the quantitative determination of glucose in the body and in fermentation fluids [1]. GOX is also used for the removal of residual glucose or oxygen from food and beverages and for the biological production of gluconic acid [2,3].

Fungal GOXs are homodimeric glycoproteins of 160 kDa with one tightly but non-covalently bound FAD cofactor per monomer. GOXs from *A. niger* and *P. amagasakiense* show 79% sequence similarity [4], are highly specific for β-D-glucose [5] and exhibit similar kinetics of glucose oxidation [6,7]. The GOX reaction proceeds through a Ping Pong mechanism [8], with the enzymes from *A. niger* and *Penicillium* species having virtually identical reaction mechanisms [8–13]. A mechanism for the whole reaction with individual rate constants in a pH-dependent scheme [11] has been proposed from a number of steady-state and transient-state kinetic analyses (reviewed in [13]). The catalytic cycle can be divided into two half-reactions, referred to as the reductive and the oxidative half-reactions (Scheme 1). In the reductive half-reaction, GOX catalyses a two-electron oxidation of β-D-glucose to δ-gluconolactone, which is hydrolysed non-enzymically to gluconic acid. The flavin ring of GOX thereby becomes reduced to $FADH_2$. Two mechanisms have been proposed for this reaction: (1) hydride transfer from substrate C-1 to flavin N-5, and (2) nucleophilic addition by the 1-OH group of β-D-glucose to the C-4a position of the flavin, followed by proton abstraction from C-1 of the substrate [11,12]. Both mechanisms are expected to be assisted by general base catalysis, with either His-516/520 or His-559/563 being the potential proton acceptor in *A. niger* and *P. amagasakiense* GOX respectively [14,15]. Thus two electrons and two protons are transferred to the flavin ($2e^-$ and $1H^+$) and to a histidine residue ($1H^+$) of the enzyme.

In the oxidative half-reaction the same two protons and two electrons are transferred from the enzyme to molecular oxygen, yielding H_2O_2 and regenerating the oxidized state of the enzyme (Scheme 1). The binding of molecular oxygen to the active site of GOX has been shown to be accompanied by the transfer of the first electron from the reduced flavin to the dioxygen, with the formation of a superoxide [16]. The second-order rate constant ($k_{cat}/K_m^{O_2}$) for the one-electron transfer to dioxygen is accelerated 100-fold at low pH by a protonated active-site histidine residue, presumably the highly conserved His-516 in *A. niger* [4], through electrostatic or hydrogen-bond stabilization of the superoxide anion intermediate [16]. This rate-limiting step is followed by subsequent electron and proton transfer steps for the formation of H_2O_2.

Despite the detailed biochemical analyses of the reaction mechanism and the identification of the active-site residues of GOX from the tertiary structures of the two enzymes [14,15], the exact roles of these residues in substrate binding still remain unclear. Moreover, there seems to be some discrepancy about the contribution of individual sugar hydroxy groups to the formation

Abbreviation used: GOX, glucose oxidase.

[1] Present address: Department of Biochemistry, Arrhenius Laboratories for Natural Sciences, Stockholm University, S-10691 Stockholm, Sweden.
[2] Present address: Universität Köln, Institut für Biochemie, Zülpicher Strasse 4, D-50674 Köln, Germany.
[3] To whom correspondence should be addressed (e-mail kalisz@gbf.de).

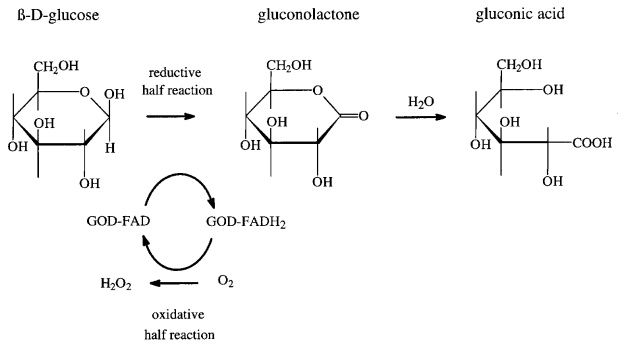

Scheme 1 Representation of the GOX reaction

The product of the reductive half-reaction, δ-gluconolactone, hydrolyses spontaneously to gluconic acid. In the oxidative half-reaction, reduced flavin is reoxidized to FAD by molecular oxygen. GOD, GOX.

of an enzyme–substrate complex [5,17]. In the present study, molecular modelling, site-directed mutagenesis and kinetic studies were performed to obtain further information about the involvement of key conserved active-site residues of *P. amagasakiense* GOX in substrate binding.

MATERIALS AND METHODS

Bacterial strains and culture conditions

P. amagasakiense (A.T.C.C. 28686), grown in potato–glucose medium at 25 °C, was used as the source of genomic DNA. *Escherichia coli* DH5α [18] was used as the host for the cloning and propagation of plasmids. *E. coli* TG2 [19] was used throughout as the host for the expression of cloned enzymes. Wild-type and mutated GOX genes were expressed in transformed *E. coli* TG2 grown at 30 °C with vigorous aeration in 1-litre batches of Luria broth medium containing 100 μg/ml ampicillin.

Plasmid construction

All recombinant DNA manipulations were performed essentially as described in [20]. The fungal gene for GOX was obtained from genomic DNA by PCR as described previously [7] and the PCR fragment was cloned directly into a pCYTEXP1 vector [7]. The resulting plasmid pPAGOX1 contained the bacteriophage λ promoters P_R and P_L in tandem, preceded by the clts857 repressor gene, the GOX coding region and the transcription terminator from the bacteriophage fd [7].

Site-directed mutagenesis

PCR-based mutagenesis with *Taq* DNA polymerase (Perkin–Elmer) was performed directly on the expression plasmid pPAGOX1. Residues Phe-418, Trp-430 and His-563 were mutated by overlap extension with two PCR runs and four oligonucleotides [21]. Mutants at positions Tyr-73, Arg-516, Asn-518 and His-520 were made by using two oligonucleotides. A cassette containing the particular mutant of GOX was exchanged with the corresponding segment of pPAGOX1. The presence of the desired mutation and the lack of second-site mutations were confirmed by DNA sequence analysis of the entire exchanged cassette by using the non-radioactive cycle sequencing method of Applied Biosystems. The data were processed on an Apple Macintosh computer.

Expression and purification of mutant derivatives of GOX

Expression of the mutant derivatives of GOX was performed with a prokaryotic expression system [7]. *E. coli* TG2, transformed with the respective mutated pPAGOX1 expression plasmid, was grown at 30 °C to a D_{600} of 0.6. Protein expression was then induced by incubation at 42 °C for a further 3 h. The cell pellet was harvested by centrifugation, resuspended in 10 mM Tris/HCl buffer, pH 8.0, and sonicated as described previously [7]. The GOX-containing inclusion bodies were centrifuged (35000 ***g***, 15 min), washed, resuspended in 2 M urea, then solubilized in 8 M urea/30 mM dithiothreitol as described previously [7]. Solubilized GOX was diluted 1:100 to a final protein concentration of 0.05–0.1 mg/ml and left to stand for 1 week at 10 °C in 20 mM Tris/HCl buffer, pH 8.0, containing 1 mM GSH, 1 mM GSSG, 0.05 mM FAD and 10% (v/v) glycerol. Refolded GOX was purified to homogeneity by mild acidification and anion-exchange chromatography on a Q-Sepharose column (Pharmacia) as described in [7]. The purified GOX mutants were dialysed against 20 mM sodium acetate, pH 6.0, and stored in liquid nitrogen.

Assays and kinetic studies

The standard assays of the wild-type and variant GOXs were performed as described previously [7] at 420 nm with 2,2′-azino-di(3-ethylbenzthiazoline-6-sulphonate) diammonium salt ('ABTS') as chromogen and 0.1 M glucose as substrate in 0.1 M sodium acetate, pH 6.0, under oxygen saturation. One unit of GOX is defined as the amount of enzyme catalysing the oxidation of 1 μmol of glucose to gluconolactone and H_2O_2 in 1 min at 25 °C. Owing to the different specific activities of the GOX variants, the amount of enzyme used varied from 5 ng to 0.2 mg per assay. Kinetic parameters were measured at a fixed concentration of oxygen (1.2 mM) and various concentrations of glucose (0.01–1.0 M). Analysis of kinetic parameters was performed by fitting the data to the Michaelis–Menten equation with the Enzfitter program [22]. The k_{cat} values were calculated per mol of native GOX (i.e. per dimer), because only the dimeric form of GOX is active.

Changes in A_{460} were followed with a Zeiss Specord spectrophotometer to test for the ability of β-D-glucose (100 mM or 1 M) or Na_2SO_3 (100 or 300 mM) to reduce enzyme-bound flavin of the inactive variants of GOX (10–20 μM). Experiments were performed under anaerobic and aerobic conditions, after flushing of all solutions with nitrogen and oxygen respectively for 5–10 min.

Protein determination

For kinetic studies and for protein purification the concentrations of GOX and soluble protein respectively were determined by amino acid analysis with an Applied Biosystems model 420A analyser. The concentration of insoluble GOX in the inclusion bodies was quantified by densitometric scanning (GT-9000 scanner; Epson) of Coomassie Blue-stained SDS/polyacrylamide gels, with the ScanPack program (Epson).

PAGE

SDS/PAGE was performed under reducing conditions with the buffer of Laemmli [23] and included a 12% (w/v) polyacrylamide running gel and a 4% (w/v) polyacrylamide stacking gel. PAGE under non-denaturing conditions (native PAGE) was performed on a Pharmacia Phast System (Amersham/Pharmacia, Freiburg,

Germany) on 10–15 % (w/v) polyacrylamide gels in accordance with the manufacturer's recommendations. The gels were stained with Coomassie Brilliant Blue-R. The isoelectric point of GOX was determined by isoelectric focusing with the Pharmacia Phast System in the pH range 4.0–6.5, as described in [24].

CD spectroscopy

CD spectra were recorded at 20 °C on a Jasco J-600 spectropolarimeter. Spectra in the near UV (300–250 nm) and far UV (250–184 nm) were recorded in cells of 0.5 and 1 mm path length and at enzyme concentrations of 0.05 and 0.1 mg/ml respectively. The CD spectra are the averages of five independent experiments on different samples of the same enzyme preparation. All spectra were corrected for the appropriate blank solutions, recorded in the absence of enzyme. The values are expressed in terms of molar ellipticity and were calculated from the observed CDs as described previously [25].

Modelling of enzyme–substrate complexes

The protein modelling package BRAGI [26] and the molecular mechanics program AMBER 4.0 [27] were used for the simulations of the enzyme–substrate complexes. A β-D-glucose molecule was docked manually into the substrate-binding pocket of *P. amagasakiense* GOX, and a series of different orientations relative to the enzyme and cofactor were energy-minimized and equilibrated by molecular dynamics calculations as described previously [15]. For all of these starting orientations the basic assumption was made that the reacting CH group should be close to the isoalloxazine moiety, and therefore the hydrogen atoms at C-1 and O-1 of glucose were directed towards the accessible acceptor atoms of FAD, His-563 Nδ1 and His-520 Nϵ2. The torsion angles of the exocyclic hydroxymethylene group C-6/O-6 of β-D-glucose were also varied in this series.

RESULTS

Structural models of enzyme–substrate complexes

In the absence of crystallographic data for enzyme–substrate complexes, modelling calculations were performed to provide an insight into the most probable position of β-D-glucose in the active site of *P. amagasakiense* GOX. Comparative force-field calculations were initially performed to analyse the protonation and orientation of His-520 and His-563 in the presence of glucose. In the first step we generated a series of structural data sets with the three possible protonation states of the nitrogen atoms Nϵ2 and Nδ1 of both histidine residues and two orientations of the His-520 side chain, whose ring was rotated for 180 ° for every protonation state. A series of different orientations of β-D-glucose relative to the enzyme and cofactor were then generated. The initial structures were generated with the hydrogen atoms at C-1 and O-1 of glucose directed towards the accessible acceptor atoms N-5 of FAD, His-563 Nδ1 and His-520 Nϵ2. Further initial structures with different torsion angles of the exocyclic hydroxymethylene group of β-D-glucose were generated to find the conformer with the lowest energy and to investigate the hydrogen bonds that might stabilize the orientation of the substrate.

The complex with the lowest energy shows only minor deviations from the X-ray structure. Only the side-chain of His-520 has to move by approx. 1.1 Å from its original position to adapt a conformation for glucose binding, which is nearly identical with the conformation of His-516 in the *A. niger* X-ray structure [15]. In the energetically most favourable system, Nδ1 of His-520 and both nitrogens of His-563 are protonated. Apart from 2-OH, every hydroxy group of β-D-glucose acts simultaneously as both hydrogen donor and acceptor in highly specific hydrogen bonds, and the 1-OH, 3-OH and 6-OH groups of β-D-glucose occupy the positions of the three crystallographic water molecules 481, 561 and 570. Consequently, 12 hydrogen bonds (9 with protein residues, 2 with water molecules and 1 with the cofactor) stabilize the orientation of β-D-glucose in the active site (Figure 1). In addition to these highly specific hydrogen bonds, the hydrophobic parts of glucose are in contact with non-polar surface areas of the protein (Tyr-73, Phe-418 and Trp-430). There is no space available for a different orientation of glucose if the basic assumption is made that the reacting 1-CH group should be close to the isoalloxazine ring. The 1-OH group is located between His-520 and His-563. The optimized distance between the hydrogen at C-1 of β-D-glucose and N-5 of the FAD cofactor is 2.4 Å. The distance between 1-OH of the substrate and the unprotonated Nϵ2 of His-520 is 2.9 Å.

Expression and purification of GOX variants in *E. coli*

Variants of *P. amagasakiense* GOX, selected on the basis of the structural and modelling information, were constructed and expressed in *E. coli* as described in the Materials and methods section. As with the wild-type protein [7], the expression of all GOX variants led to the formation of insoluble inclusion bodies. Quantification of the expression levels of GOX by densitometric scanning of Coomassie Blue-stained SDS/polyacrylamide gels demonstrated each GOX variant to represent over 50 % of the total cellular protein fraction (results not shown). No enzymic activity was detected in either the soluble or the insoluble fraction.

Reconstitution of GOX variants was performed as described in the Materials and methods section. Refolding of most GOX variants could be followed by measuring increases in enzyme activity. The kinetics of GOX reactivation followed an apparent single first-order reaction, identical with that observed for the wild-type enzyme [7]. Because optimal refolding was observed under identical conditions for all variants with measurable activity, the same reconstitution method was used for the reactivation of variants with no detectable activity. All reconstituted GOX variants were purified to homogeneity by mild acidification and ion-exchange chromatography as described in the Materials and methods section. The yields of the variants ranged from 5 to 15 mg per litre of *E. coli* culture. These quantities were very similar to the 12.5 mg/l obtained with the wild-type GOX [7]. The differences in the yields can be attributed to the mild acidification step, which caused the aggregation of 20–50 % of the GOX variants. No attempt was made to modify or eliminate this step, because it allowed the separation of correctly folded GOX from incorrectly folded enzyme [7].

Structural characterization of GOX variants

The structures of variant and wild-type proteins were compared by CD spectroscopy. With the exception of the W430N and Y73Q mutants, the CD spectra of all GOX proteins were virtually identical (results not shown), implying identical α-helix contents and indicating that the variant enzymes had adopted a similar conformation to that of the wild-type GOX. Consequently, variants Y73Q and W430N were not studied further, whereas the other variant preparations were considered to be suitable for investigating the effect of the mutations on localized alterations in the active site.

All variant enzymes migrated under identical conditions as a single sharp band with apparent molecular masses of 60 and 120 kDa in SDS/PAGE and native PAGE respectively (results

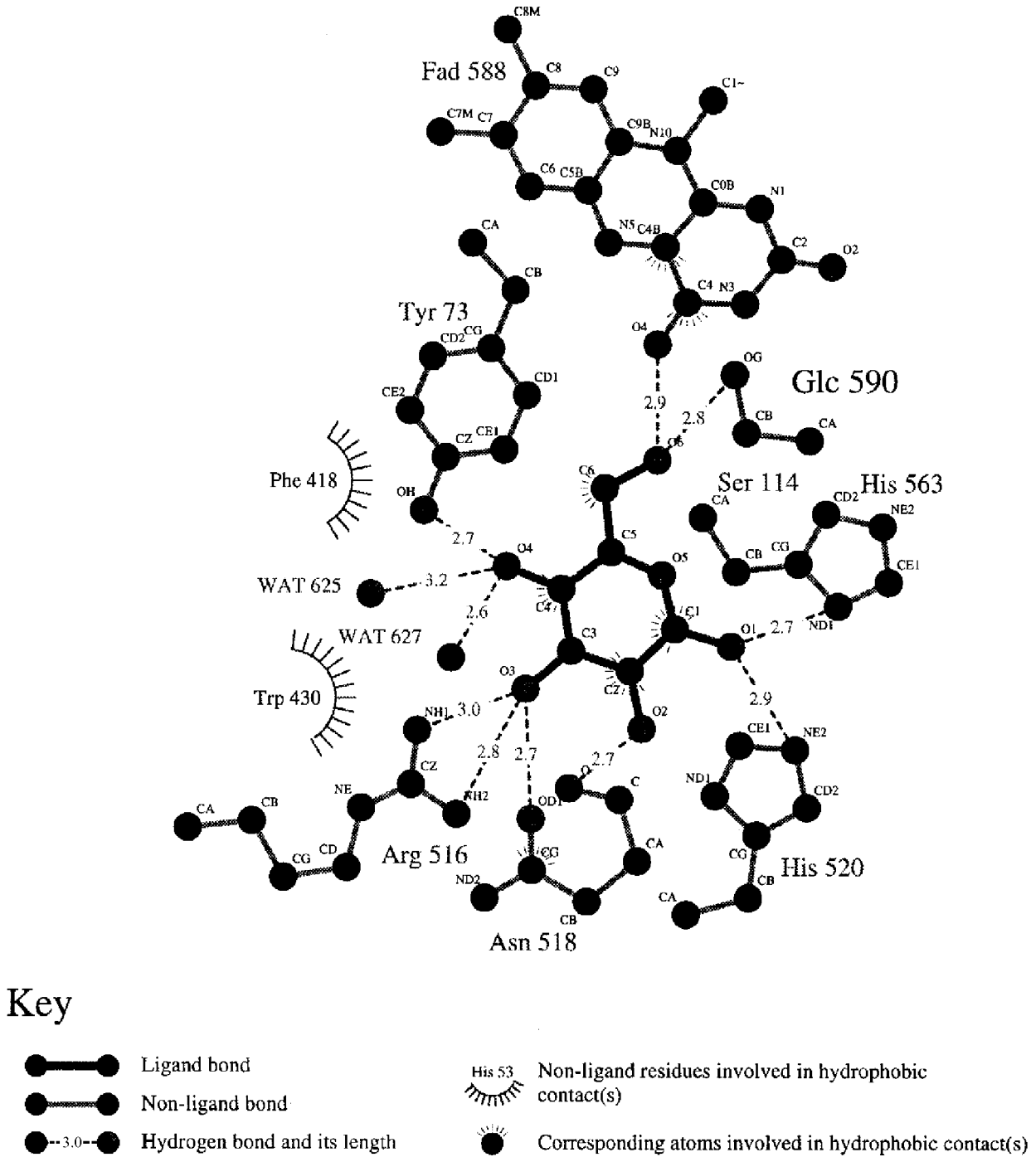

Figure 1 Diagram (LIGPLOT [34]) of the hydrogen bonds and hydrophobic interactions of the modelled substrate β-D-glucose with active-site residues in wild-type *P. amagasakiense* GOX

The hydrogen bond of 3.3 Å between the backbone Gly-112 and 6-OH of β-D-glucose has been omitted from this representation. WAT, water.

not shown). Further, the UV/visible absorption spectra (180–600 nm) of the variant enzymes compared favourably with those of authentic GOX, with maxima at 260, 370 and 460 nm (results not shown). The identical physicochemical properties of the wild-type and variant GOXs implies that all variants were expressed at full length and correctly folded, with dimerization being only possible with the proper incorporation of the cofactor in the FAD-binding pocket and the correct folding of GOX [7,28,29].

Catalytic activity of variant GOX forms with β-D-glucose

The effect of the substitution on the steady-state kinetics of glucose oxidation is shown in Table 1. With the exception

Table 1 Kinetic parameters of *P. amagasakiense* GOX variants for the oxidation of β-D-glucose at pH 6

Initial rates of glucose oxidation were determined at 25 °C in 0.1 M sodium acetate buffer, pH 6.0, at a fixed oxygen concentration of 1.2 mM, as described in the Materials and methods section. Kinetic parameters were analysed with the Enzfitter program [22]. The relative rate (specificity) of glucose oxidation was calculated from the equation $v_{variant}/v_{wild\text{-}type} = (k_{cat}^{variant}/K_m^{variant})/(k_{cat}^{wild\text{-}type}/K_m^{wild\text{-}type})$. Errors are shown as ±S.D. Abbreviation: n.d., not detectable.

GOX variant	V_{max} (units/mg)	K_m (app) (mM)	k_{cat} (s^{-1})	k_{cat}/K_m ($mM^{-1} \cdot s^{-1}$)	$10^3 \times$ Specificity (variant/wild-type)
Wild type	926 ± 9	6.2 ± 0.5	2003	323	(1000)
Y73F	295 ± 4	24 ± 2	639	26	80.5
F418A	6.6 ± 0.2	78 ± 7	14	0.2	0.6
F418V	147 ± 1	13.3 ± 0.7	318	24	74.3
W430A	10.5 ± 0.3	27 ± 4	23	0.8	2.5
R516K	279 ± 30	513 ± 90	603	1.2	3.7
R516Q	33 ± 2	733 ± 67	71	0.1	0.3
N518T	539 ± 8	36 ± 2	1166	33	102.2
H520A	0.08 ± 0.001	5.8 ± 0.7	0.16	0.03	0.1
H520V	0.01 ± 0.001	6.7 ± 0.9	0.03	0.004	0.01
H563A	n.d.	n.d.	–	–	–
H563V	n.d.	n.d.	–	–	–

of variants H563A and H563V, which were inactive, all variants exhibited at least trace amounts of activity. In contrast with wild-type GOX, which like the *A. niger* GOX [30,31] demonstrates a high reactivity with sulphite, the His-563 variants were unable to react with sodium sulphite. Hence the complete loss of activity of these variants seems to be due to a loss of activation of the flavin ring through the removal of the His-563 residue [30].

Although variants H520A and H520V were almost completely inactive (less than 0.2% of the wild-type activity), their affinity for β-D-glucose (i.e. the apparent K_m) was virtually unaffected. In fact, most of the substitutions effected decreases to less than one-tenth in the V_{max} of the reaction, but they did not affect the apparent affinity for β-D-glucose more than 6-fold. The only exceptions were variants F418A and R516Q, which showed at least 10-fold higher apparent K_m values and exhibited V_{max} values at most one-tenth those of wild-type GOX. In contrast, the maximum velocities of variants Y73F, F418V, R516K and N518T were only slightly affected. However, a comparison of the specificities of the variants, using the equation:

$$v_{variant}/v_{wild\text{-}type} = (k_{cat}^{variant}/K_m^{variant})/(k_{cat}^{wild\text{-}type}/K_m^{wild\text{-}type})$$

demonstrates that all of the substitutions had a detrimental effect on the specificity for glucose (Table 1). Substitutions Y73F and F418V affected the specificity for glucose by only one order of magnitude. All other variants demonstrated 2–3 orders of magnitude lower specificities than wild-type GOX, whereas the specificities of the His-520 variants decreased by $1/10^4$ to $1/10^5$.

DISCUSSION

GOX catalyses the oxidation of β-D-glucose by molecular oxygen to δ-gluconolactone and H_2O_2. A mechanism for the GOX reaction has been proposed after numerous steady-state and transient-state kinetic analyses [8–13]. The enzyme is highly specific for β-D-glucose [5], with more than 5-fold faster maximum velocities and at least 20-fold higher apparent K_m values than for other sugars [5–7]. However, despite several biochemical studies [5,27] and the availability of the three-dimensional structures of GOX from *A. niger* and *P. amagasakiense* [14,15], crystallographic data for an enzyme–substrate complex are not available and the exact roles of the active-site residues in substrate binding and/or glucose oxidation have not been clarified.

In the present study we have determined the roles of key conserved active-site residues of *P. amagasakiense* GOX in the binding of β-D-glucose by molecular modelling, site-directed mutagenesis and kinetic studies. Variant proteins were produced by controlled refolding *in vitro* of insoluble polypeptides after expression in *E. coli* and purified to electrophoretic homogeneity. Similarities in the electrophoretic behaviour, absorption and CD spectra of the recombinant and variant enzymes indicated correct folding, dimerization and the adoption of similar conformations [28,29]. Thus any observed differences in the kinetic properties of the variants can be attributed to changes in hydrogen-bonding and/or hydrophobic interactions between the substituted residue and the substrate.

In the modelled *P. amagasakiense* GOX complex the 1-OH group of β-D-glucose is located almost equidistantly between the two catalytic histidine residues and forms a hydrogen bond to Nε2 of His-520 and Nδ1 of His-563 (Figure 1). Substitution of His-520 results in a decrease in V_{max} of $1/10^4$ to $1/10^5$ without affecting the apparent K_m for β-D-glucose. Replacement of His-563 causes the complete inactivation of GOX. Both the active-site histidine residues could act in the reaction mechanism as a general base in the reductive half-reaction and as general acid in the oxidative half-reaction; each of the two histidine residues has been proposed for this role [14,15]. However, results in the present study show that not just one but both histidine residues are probably involved in the glucose oxidation reaction. His-563 most probably has an important role in FAD activation [30,31] and/or hydride transfer from glucose C-1 to flavin N-5 [11,12], whereas His-520, which is highly conserved in the glucose-methanol-choline oxidoreductase family [4,32], might indeed be involved in electron transfer to dioxygen from reduced flavin [16]. However, further work is required to determine the exact roles of the two catalytic histidine residues in the GOX reaction mechanism.

Asn-518 forms hydrogen bonds to the 2-OH and 3-OH groups of β-D-glucose in the model complex. Variant N518T demonstrates only a slightly decreased V_{max} and an apparent K_m 80% lower, showing a specificity for glucose one-tenth that of the wild type. Molecular modelling shows the side-chain of the substituted threonine residue to be fixed by the hydroxy group of Thr-335, with the methyl group of Thr-518 pointing towards the substrate-binding pocket. The hydrogen bond to the 2-OH group of glucose is consequently lost, although the 3-OH group of the

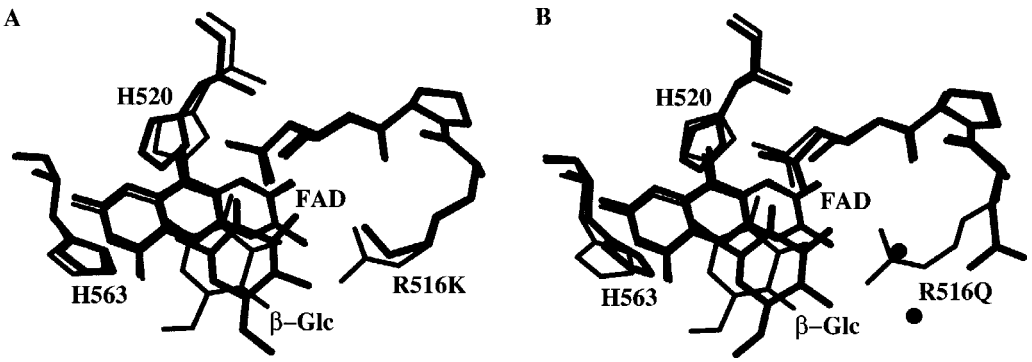

Figure 2 Active sites of the Arg-516 variants and wild-type GOX from *P. amagasakiense* with the modelled β-D-glucose (β-Glc)

The models were produced with BRAGI [26] and rendered with POV-Ray. Residues of the energy-minimized model complex of the wild-type GOX are shown in thin lines. The superimposed complex models of the R516K (**A**) and R516Q (**B**) variants are shown in thick lines. The two water molecules that moved during the molecular dynamics simulation between the β-D-glucose and the Gln-516 side chain are shown as dark spheres.

sugar remains hydrogen-bonded to the backbone carbonyl of Thr-518. This leads to the positioning of the 1-CH group of glucose at a less favourable distance and angle to the N-5 of FAD than in the wild type, which might explain the lower specificity of the N518T variant. However, these results demonstrate that the 2-OH group of glucose has only a minor role in the binding of glucose to the active site of GOX. This is in accordance with previous observations [17] and might explain the similar apparent K_m values of GOX for 2-deoxy-D-glucose and β-D-glucose [5,7].

Arg-516 forms two hydrogen bonds with its terminal amino groups to the 3-OH group of D-glucose (Figure 1). Both of its variants (R516K and R516Q) exhibit significantly lower affinities for the sugar than the wild type. As shown by molecular modelling, a lysine residue at position 516 can still form a hydrogen bond with its side-chain to the 3-OH group of glucose (Figure 2A). Glutamine, in contrast, cannot interact directly with the sugar, although it can still interact indirectly with glucose via a water molecule (Figure 2B). Replacement of Arg-516 with a lysine already causes a decrease in the specificity for glucose to 1/275. The additional disruption of the hydrogen bonds to the 3-OH group of glucose through an R516Q substitution not only further increases the apparent K_m for glucose, but simultaneously significantly decreases the maximum velocity, effecting a decrease in the specificity for glucose to 1/3400. Molecular modelling demonstrates changes in the position of glucose in the active site of the two Arg-516 variants, with the 1-CH and 1-OH groups being positioned farther away and at less favourable angles to the N-5 of FAD and the catalytic histidines respectively than in the wild type (Figure 2). These changes in the position of glucose consequently lead to a decrease in the maximum rates of glucose oxidation. None of the other substitutions effected similar changes in the distance of the reacting group of glucose to the catalytic site. Thus the formation of hydrogen bonds between the 3-OH group of glucose and the two side-chain amino groups of Arg-516 seems to be the dominant step in the binding of the substrate in the active site of GOX. These results corroborate the findings of Pazur and Kleppe [5], who reported an equatorially orientated hydroxy group at position 3 as a possible site of combination of glucose with GOX. Moreover, they provide an explanation for the 1/130 affinity and four orders of magnitude lower specificity of GOX for D-allose than for glucose [33]: the 3-epimer is unable to form the necessary hydrogen bonds to Arg-516.

The 4-OH group of glucose is hydrogen-bonded to Tyr-73 and also interacts with two vicinal water molecules. The substitution Y73F results in a loss of the hydrogen bond with Tyr-73 but retains the hydrophobic environment for the non-polar region of glucose. This results in only minor changes in the apparent K_m and V_{max} values. In accordance with the kinetic results, no significant changes are observed in the position of glucose in the Y73F variant. Thus, in contrast with the findings of Sierks et al. [17], our results imply that a hydrogen bond between residue 73 and the 4-OH group of glucose does not have an important role in the binding of the substrate to GOX. However, the apparent loss of secondary structure by the Y73Q variant demonstrates the importance of a hydrophobic group in this position to provide a hydrophobic environment for glucose C-6 and/or FAD C7M.

The orientation of glucose is further stabilized by hydrophobic contacts to Phe-418, which interacts with the exocyclic methylene group of glucose, and Trp-430. Both residues also interact with Glu-416, Asn-518 and His-563. An exchange of either of these residues for alanine creates a large gap near the catalytic residues and seems to cause minor changes in the angles of the 1-CH and 1-OH groups of glucose to the plane of the flavin ring and the catalytic histidine residues respectively. These conformational changes explain the observed decreases in V_{max} of 1/90 to 1/140 but only 4–12-fold increases in the apparent K_m values of these variants. Consequently, the specificities of the W430A and F418A variants for glucose are 1/400 and 1/1600 respectively of the wild type. Interestingly, wild-type GOX also exhibits a specificity for D-xylose, which lacks the exocyclic methylene group, that is 1/1600 that for D-glucose [7] and demonstrates a less favourable angle between 1-CH of xylose and N-5 of FAD [15]. However, although GOX exhibits a 60-fold higher affinity for glucose than for xylose [7], replacement of Phe-418 affects the maximum velocity of glucose oxidation more than the affinity for the substrate.

In conclusion, β-D-glucose is stabilized in the active site of GOX by a network of 12 highly specific hydrogen bonds: 9 with protein residues, 2 with water molecules and 1 with the cofactor. In addition to the hydrogen-bond network, hydrophobic contacts to Phe-418, Trp-430 and to a smaller extent Tyr-73 stabilize β-D-glucose in the active site of GOX. Each of the catalytic histidine residues forms a hydrogen bond with the 1-OH group of glucose; both residues seem to have an active role in the reaction mechanism of GOX. However, the critical factor in determining

the efficient binding of β-D-glucose by GOX seems to be the interaction between the 3-OH group of the substrate and Arg-516 of the enzyme through two hydrogen bonds. These results corroborate the findings of Pazur and Kleppe [5], who identified the 3-OH group of glucose as being the most important structural element for substrate binding. The other active-site residues contribute to a smaller extent to the efficient binding of glucose.

We thank Professor M. Singh (GBF) for helpful discussions.

REFERENCES

1 Wilson, R. and Turner, A. P. F. (1992) Biosens. Bioelectr. **7**, 165–185
2 Röhr, M., Kubicek, C. P. and Kominek, J. (1983) in Biotechnology, vol. 3 (Rehm, H.-J. and Reed, G., eds.), pp. 455–465, Verlag Chemie, Weinheim
3 Crueger, A. and Crueger, W. (1984) in Biotechnology, vol. 6a (Rehm, H.-J. and Reed, G., eds.), pp. 421–457, Verlag Chemie, Weinheim
4 Kiess, M., Hecht, H.-J. and Kalisz, H. M. (1998) Eur. J. Biochem. **252**, 90–99
5 Pazur, J. H. and Kleppe, K. (1964) Biochemistry **3**, 578–583
6 Kalisz, H. M., Hendle, J. and Schmid, R. D. (1997) Appl. Microbiol. Biotechnol. **47**, 502–507
7 Witt, S., Singh, M. and Kalisz, H. M. (1998) Appl. Environ. Microbiol. **64**, 1405–1411
8 Gibson, Q. H., Swoboda, B. E. P. and Massey, V. (1964) J. Biol. Chem. **239**, 3927–3934
9 Nakamura, S. and Ogura, Y. (1962) J. Biochem. (Tokyo) **52**, 214–220
10 Nakamura, S. and Ogura, Y. (1968) J. Biochem. (Tokyo) **63**, 308–316
11 Bright, H. J. and Appleby, M. (1969) J. Biol. Chem. **244**, 3625–3634
12 Weibel, M. K. and Bright, H. J. (1971) J. Biol. Chem. **246**, 2734–2744
13 Bright, H. J. and Porter, D. J. T. (1975) The Enzymes, 3rd edn, vol. 12, pp. 421–505, Academic Press, New York
14 Hecht, H.-J., Kalisz, H. M., Hendle, J., Schmid, R. D. and Schomburg, D. (1993) J. Mol. Biol. **229**, 153–172
15 Wohlfahrt, G., Witt, S., Hendle, J., Schomburg, D., Kalisz, H. M. and Hecht, H. J. (1999) Acta Cryst. Sect. D: Biol. Crystallogr. **55**, 969–977
16 Su, Q. and Klinman, J. P. (1999) Biochemistry **38**, 8572–8581
17 Sierks, M. R., Bock, K., Refn, S. and Svensson, B. (1992) Biochemistry **31**, 8972–8977
18 Hanahan, D. (1985) in DNA Cloning, vol. 1 (Glover, D. M., ed.), pp. 109–135, IRL, Oxford
19 Gibson, T. J. (1984) Ph.D. Thesis, University of Cambridge, U.K.
20 Sambrook, J., Fritsch, E. F. and Maniatis, T. (1989) Molecular Cloning: A Laboratory Manual, 2nd edn, Cold Spring Harbor Laboratory, Cold Spring Harbor, NY
21 Ho, S. N., Hunt, H. D., Horton, R. M., Pullen, J. K. and Pease, L. R. (1989) Gene **77**, 51–59
22 Leatherbarrow, R. J. (1987) Enzfitter, Imperial College of Science and Technology, London
23 Laemmli, U.K. (1970) Nature (London) **227**, 680–685
24 Butcher, L. A. and Tomkins, J. K. (1985) Anal. Biochem. **148**, 384–388
25 Hennessey, Jr, J. P. and Johnson, Jr, W. C. (1981) Biochemistry **20**, 1085–1094
26 Schomburg, D. and Reichelt, J. (1988) J. Mol. Graph. **6**, 161–165
27 Pearlman, D. A., Case, D. A., Caldwell, J. C., Seibel, G. L., Singh, U. C., Weiner, P. and Kollman, P. A. (1991) AMBER 4.0, University of California, San Francisco
28 Swoboda, B. E. P. (1969) Biochim. Biophys. Acta **175**, 365–379
29 Tsuge, H. and Mitsuda, H. (1971) J. Vitaminol. **17**, 24–31
30 Swoboda, B. E. P. and Massey, V. (1966) J. Biol. Chem. **241**, 3409–3416
31 Massey, V. and Hemmerich, P. (1980) Biochem. Soc. Trans. **8**, 246–256
32 Cavener, D. R. (1992) J. Mol. Biol. **223**, 811–814
33 Witt, S. (1996) Ph.D. Thesis, University of Hanover, Germany
34 Wallace, A. C., Laskowski, R. A. and Thornton, J. M. (1995) Protein Eng. **8**, 127–134

Received 30 November 1999/21 January 2000; accepted 15 February 2000